

RESEARCH ARTICLE



Cite this: *Org. Chem. Front.*, 2026, **13**, 54

Received 9th September 2025,
Accepted 18th October 2025
DOI: 10.1039/d5qo01285f
rsc.li/frontiers-organic

Are N-heterocyclic carbene radical cations relevant intermediates in radical transformations?

Preslav Smits,^a Ludivine Delfau,^a Sheima Bougoffa,^a Florian Molton,^a Jacques Pecaut,^b Julie Broggi,^{c,d} Eder Tomás-Mendivil^a and David Martin^a

N-Heterocyclic carbene (NHC) radical cations have been increasingly hypothesized as key intermediates in NHC-promoted radical reactions, but have eluded direct observation so far. Herein, we report joint experimental and theoretical efforts to assess the issues surrounding the possible existence, generation and observation of these postulated species. We show that they are unlikely to be the relevant intermediates in most NHC-promoted radical reactions.

Introduction

For the last decades, stable N-Heterocyclic Carbenes (NHCs) **1** have stood out as handleable reagents, efficient ligands and original synthetic building blocks.¹ Recent developments in radical NHC-catalysis have drawn attention to the corresponding NHC radical cations **1⁺** as possible key intermediates.² Despite the convenience of these radicals for proposing catalytic cycles, they have eluded spectroscopic observation so far³ and evidence for their genuine involvement remains indirect and tenuous.

Yet, radicals **1⁺** should be readily accessible through oxidation of the corresponding NHC.⁴ Indeed, imidazol-2-ylidenes **1a–b** perform the stoichiometric reduction of ferricenium⁵ (*E* = +0.38 V vs. SCE) and trityl (*E* = +0.27 V vs. SCE) cations (Fig. 1a).^{6,7} Cyclic alkylaminocarbene (CAAC) **1c**^{3,8} and mesoionic carbene (MIC) **1d**⁹ were used for the one electron-reduction of iminium derivatives and quinones, respectively. Although these reactions involved the formal oxidation of a free NHC **1** and should lead to the generation of corresponding radical cation **1⁺**, only the formation of azolium salts **1·H⁺** was observed. This suggested that H⁺ abstraction from solvent molecules by **1⁺** is very fast. However, even the formation of **1·H⁺** does not necessarily imply the formation of **1⁺** by single electron transfer (SET). Indeed, Song and Lee revisited the reaction of trityl cation with **1a**, which affords **1a·H⁺** and triphenylmethane. Their DFT study unveiled an alternative mechanism involving **1a**–trityl cation adduct¹⁰ in place of the initially proposed SET with formation of **1⁺** and

trityl radicals.⁶ Interestingly, Clyburne *et al.* reported that the oxidation of **1b** with tetracyanoethylene led to the formation of dicationic dimer **2b²⁺**, resulting either from direct dimerization of radical cation **1b⁺**, or (more likely) from its reaction with **1** to produce **2b⁺** which was then oxidised to afford **2b²⁺** (Fig. 1b).⁵

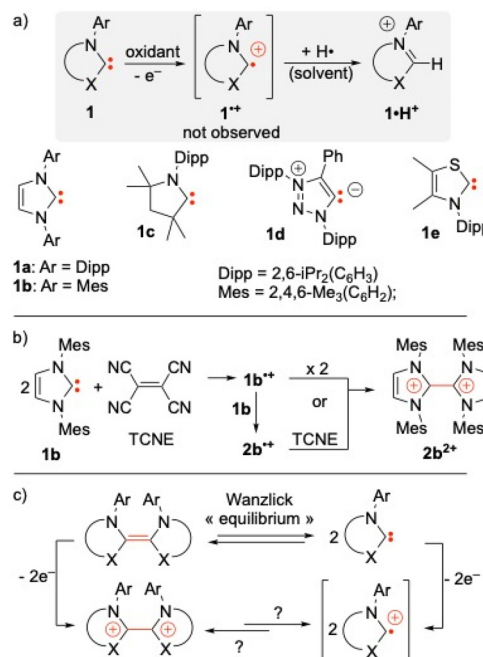


Fig. 1 (a) Oxidation of N-heterocyclic carbenes **1**, putative formation of the corresponding radical cation **1⁺** and subsequent H⁺ abstraction to afford azolium **1·H⁺**. (b) Formation of dicationic dimer **2b²⁺** upon oxidation of **1b** with tetracyanoethylene (TCNE). (c) Oxidized version of the Wanzlick equilibrium as a possible source of NHC radical cations.

^aUniv. Grenoble Alpes, CNRS, DCM, 38000 Grenoble, France.

E-mail: david.martin@univ-grenoble-alpes.fr

^bUniv. Grenoble Alpes, CEA, CNRS, INAC-SyMMES, 38000 Grenoble, France

^cAix Marseille Univ., CNRS, ICR - UMR 7273, 13005 Marseille, France

^dInstitut universitaire de France (IUF), France



Dimers 2^{2+} could constitute a reservoir for transient radicals 1^{+*} (Fig. 1c), similarly to olefins 2 (the reduced forms of dicationic $2b^{2+}$), which have been used as sources of NHC ligands long before the advent of stable NHCs 1.^{11–13} The formal relationship between 1 and their dimers 2 is well-known as the Wanzlick equilibrium.^{11,14} Note that a genuine equilibrium has been evidenced for benzimidazolylidenes only.¹⁵

In fact, the Wanzlick equilibrium is fully shifted towards the free carbene in the case of electron-rich aromatic heterocycles (typically: imidazol- and triazol-ylidenes).¹⁶ Conversely, the dimerization of saturated and/or more electrophilic NHC (imidazolidinylidenes, thiazolylidenes, CAAC, etc.) is thermodynamically favoured, unless high steric demand around the carbene centre prevents it. Importantly, in the absence of acid catalyst, the formation of the dimer 2 is significantly slowed, to the point that even metastable NHC with smaller substituents can be isolated prior to their dimerization.¹⁷ In contrast with the well-studied Wanzlick equilibrium, the potential of dicationic dimers 2^{2+} as sources of radical 1^{+*} has never been considered: their reactivity studies have been confined to their redox relation to electron donors 2¹⁸ and their anecdotal conversion to ureas.¹⁹

Herein, we report our experimental and theoretical efforts to assess the issues surrounding the possible existence and generation of elusive NHC radical cations. We examined: (i) whether a tuning of substituents can allow for the stabilization and observation of a NHC radical cation and, conversely, (ii) whether transient NHC radical cations 1^{+*} could be generated from the homolytic dissociation of dicationic 2^{2+} . In other words, we probe for the possibility of an oxidized equivalent to the Wanzlick equilibrium.

Results and discussion

Evaluation of the stabilization of NHC radical cations

Jana *et al.* observed an EPR signal when monitoring the reaction of CAAC **1c** with $\text{NO}\cdot\text{BF}_4$.^{3b} The authors initially attributed the $1:1:1$ triplet to the CAAC radical cation $1c^{+*}$, but they later invalidated this interpretation on the basis of MINDO calculations.^{3a} Interestingly, they found that H^{\cdot} abstraction from solvents by radical $1c^{+*}$ was highly exothermic, supporting further the high reactivity and elusiveness of this radical. The stability of organic radicals is commonly expressed using isodesmic H-transfer reactions. In particular, the enthalpy of H-abstraction from methane to afford methyl radical is regarded as a standard metric for radical stabilisation energy (RSE) for C-centred radicals.²⁰

We computed the RSE of radicals **1a–e**⁺ at the B3LYP-GD3(BJ)/def2svp level of theory (see Fig. 2).²¹ We found negative values, indicating stabilities even lower than that of the methyl radical. This was unsurprising, since **1a–e**⁺ are non-conjugated electron-poor carbon-centred radicals that are destabilized by the $-\text{I}$ electronic effect of the amino groups. In line with this reasoning, CAAC-based radical $1c^{+*}$ was found less

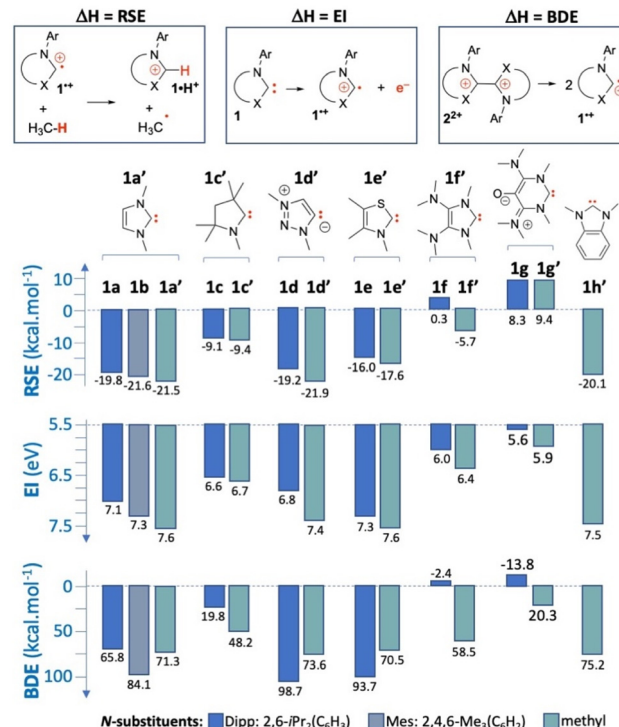


Fig. 2 Computed (B3LYP-GD3(BJ)/def2svp) enthalpy of hydrogen atom exchange between methane and 1^{+*} (RSE), ionization energy of NHC 1 (IE) and enthalpy of homolytic bond dissociation of dimers 2^{2+} (BDE).

unstable because of the replacement of an amino with an electron-donating alkyl group, resulting in an RSE of $-9.4 \text{ kcal mol}^{-1}$, instead of about $-20 \text{ kcal mol}^{-1}$ for **1a–b**⁺ and **1d–e**⁺. RSE correlates well with the inverses of ionization energy (IE) of NHC 1 and bond dissociation enthalpy of 2^{2+} , which could be considered as alternative metrics for the stability of radicals 1^{+*} (Fig. 2). Importantly, despite their bulky 2,6-di(isopropyl) phenyl (Dipp) or 2,4,6-trimethylphenyl (Mes) groups, enthalpies of dimerization of **1a–e**⁺ (BDE) remain very high, especially when considering that their reduced forms **1a–e** are stable as free NHC and do not dimerize.

When decreasing steric hindrance with small methyl N-substituents (model NHCs **1f–g**) enthalpies of dimerization did not increase significantly and trends in relative stability remained unchanged.

Next, we turned to electron-enriched NHCs **1f**²² and **1g**²³ which feature bis(dimethylamino)ethylene and bis(dimethylamino) oxyallyl patterns, respectively (Scheme 1). The redox-active patterns resulted in positive RSE of 0.3 and 8.3 kcal



Scheme 1 Mesomeric limit forms of NHC radical cations **1f**⁺ and **1g**⁺.



mol^{-1} (-5.4 and $+9.4$ kcal mol^{-1} for methyl substituted $\mathbf{1f}^{\bullet+}$), respectively. These values still correspond to highly reactive radicals. As a comparison, at this level of theory, RSE for phenyl ($\text{C}_6\text{H}_5^{\bullet}$), *tert*-butyl ($\text{C}_4\text{H}_9^{\bullet}$) and allyl ($\text{C}_3\text{H}_5^{\bullet}$) radicals are -7.5 , $+11.3$ and $+19.5$ kcal mol^{-1} respectively, whereas radical HC(O)C(H)NH_2 , featuring stabilizing capto-dative substitutions, has a RSE of $+32.1$ kcal mol^{-1} (Fig. 3).

Nevertheless, $\mathbf{1f}^{\bullet+}$ and $\mathbf{1g}^{\bullet+}$ are very different in nature from localized radicals $\mathbf{1a-e}^{\bullet+}$. DFT calculations indicated that the spin density of $\mathbf{1f}^{\bullet+}$ and $\mathbf{1g}^{\bullet+}$ is spread over the redox-active pattern, with only 19% and 10% Mulliken spin density on the former carbene centre, respectively (Fig. 4a). Furthermore, in contrast to NHCs **1a-f**, the HOMO of the electron-rich NHC **1g** is not the lone pair of the carbene (HOMO-1), but a π -orbital of the oxyallyl system (Fig. 4b). In the case of **1f**, both molecular orbitals are close in energy. From an experimental point of view, 1,3-bis(dimethylamino)oxyallyl,²⁴ as well as di(amino)ethylene radical cations^{4b,25} often display a remarkable stability. In particular, the one-electron oxidation of adducts of NHC **1f** and **1g** can lead to stable or persistent radical cations.^{22,23} Overall, we considered that chances were fair that $\mathbf{1f}^{\bullet+}$ and $\mathbf{1g}^{\bullet+}$ could be generated and observed.

Attempts to observe stabilized NHC radical cations

We synthesized NHC **1f** in an electrochemical cell by adding 1.1 equivalent of potassium bis(trimethylsilyl)amide to a THF

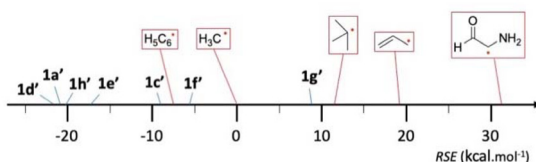


Fig. 3 Comparative stabilities of methyl *N*-substituted NHC radical cations on the RSE scale.

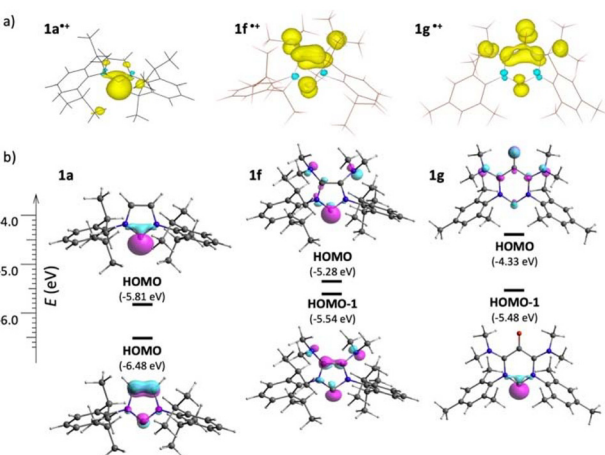


Fig. 4 (a) Representation of Mulliken spin density of NHC radical cations $\mathbf{1}^{\bullet+}$, $\mathbf{1f}^{\bullet+}$ and $\mathbf{1g}^{\bullet+}$. (b) Representation of HOMO and HOMO-1 of the corresponding NHCs.

solution of $\mathbf{1f} \cdot \mathbf{H}^+$ and 0.1 M $[\text{Bu}_4\text{N}]^+\text{PF}_6^-$. The corresponding cyclic voltammograms featured an irreversible oxidation wave at about $+0.8$ V *versus* SCE (Fig. 5). A second reversible oxidation was observed at about $+1.3$ V, which corresponded to the one-electron oxidation of precursor $\mathbf{1f} \cdot \mathbf{H}^+$ to radical $\mathbf{1f} \cdot \mathbf{H}^{\bullet+}$. Therefore, we concluded that the oxidation of **1f** afforded a transient radical $\mathbf{1f}^{\bullet+}$, which underwent a fast H[•] abstraction to yield imidazolium $\mathbf{1f} \cdot \mathbf{H}^+$, similarly to non-stabilized NHC radical cations **1a-e**^{•+}.

In contrast, the cyclic voltammogram of **1g** in a 0.1M $[\text{Bu}_4\text{N}]^+\text{PF}_6^-$ THF solution featured a pseudo-reversible oxidation wave at about -0.5 V *versus* SCE (Fig. 6a). We performed the electrolysis of the solution at -0.3 V. UV-vis monitoring indicated the formation of an intermediate featuring an absorption in the

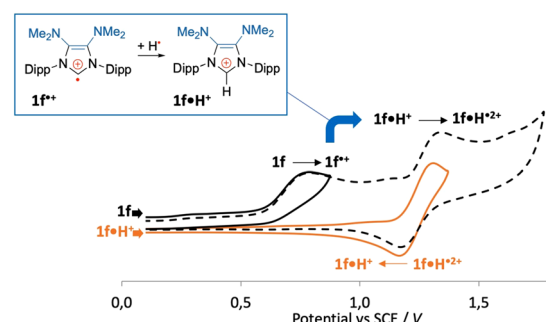


Fig. 5 Cyclic voltammograms of **1f** (black) and $\mathbf{1f} \cdot \mathbf{H}^+$ (orange) in THF + 0.1M $[\text{Bu}_4\text{N}]^+\text{PF}_6^-$, scan rate: 10 mV s⁻¹.

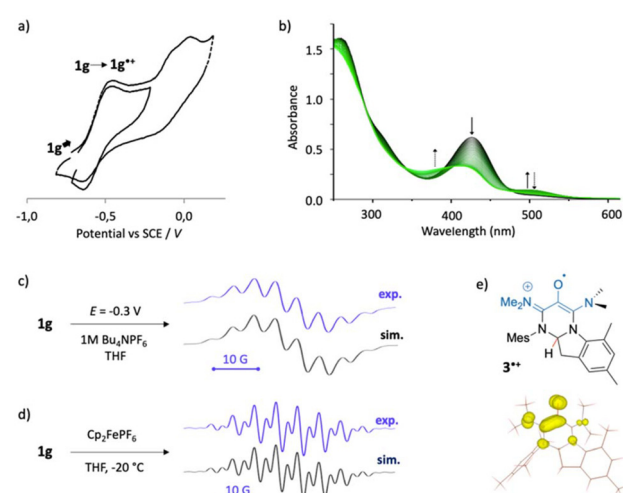


Fig. 6 (a) Cyclic voltammograms of **1g** in THF + 0.1M $[\text{Bu}_4\text{N}]^+\text{PF}_6^-$, scan rate: 100 mV s⁻¹. (b) UV monitoring of electrolysis at $E = -0.3$ V *vs.* SCE. (c) Resulting experimental X-band isotropic EPR spectrum and corresponding simulated spectrum with Lorentzian line-broadening parameter $L_w = 0.3$, $a^{14}\text{N} = 6.5$ MHz (2 nuclei), $a^1\text{H} = 12.0$ MHz (1 nucleus) and 14.0 MHz (6 nuclei). (d) EPR of a solution of **1g** in THF upon addition of Cp_2FePF_6 , corresponding simulated spectrum with $L_w = 0.2$, $a^{14}\text{N} = 6.7$ MHz (2 nuclei), $a^1\text{H} = 11.7$ MHz (1 nucleus) and 14.0 MHz (6 nuclei). (e) Proposed formation of oxyallyl radical $\mathbf{3}^{\bullet+}$ and representation of computed Mulliken spin density.



typical region for oxyallyl radical cations, at 495 nm (Fig. 6b). X-band EPR of an aliquot confirmed the formation of a radical, which could be observed for a few minutes at room temperature (Fig. 6c). However, the EPR spectrum couldn't correspond to radical **1g**⁺. Indeed, the hyperfine structure displayed an even number of bands and, therefore, corresponded to an odd number of coupled atomic spins of $\frac{1}{2}$ (protons). Accordingly, the experimental spectrum could be simulated by considering a 12.0 MHz coupling with an isolated proton, in addition to 6 equivalent protons (14.0 MHz) and 2 nitrogen atoms (6.5 MHz).²⁶

Considering the tendency of electron-poor N-heterocyclic carbene centres to undergo intramolecular C–H insertion,²⁷ we hypothesized that the oxidation of **1g** triggered a C–H insertion into a methyl group of a mesityl *N*-substituent to afford oxyallyl radical cation **3**⁺ (Fig. 6e). Our assumption was further supported by DFT calculations (B3LYP-GD3(BJ)/def2svp), which indicated that the isomerization of **1**⁺ into **3**⁺ was highly exergonic ($\Delta G = -33$ kcal mol⁻¹). Importantly, the conjugation of one (dimethyl)amino group with the oxyallyl system of **3**⁺ is prevented by steric constraints from the polycyclic structure. As a consequence, the spin density of **3**⁺ is concentrated on one side of the 6-membered heterocycle and significant hyperfine couplings (B3LYP/EPR-III) are limited to a few atoms: the proton at the former carbene centre ($a_{\text{DFT}} = 15$ MHz), two nitrogen atoms ($a_{\text{DFT}} = 9$ and 8.6 MHz) and six protons of a dimethyl amino group ($a_{\text{DFT}} = 11$ MHz). These values fit well with experimental data, in contrast with computed hyperfine couplings for **1g**⁺ ($a_{\text{DFT}} = 9$ MHz with two ¹⁴N and 13 MHz with 12 protons).

We also performed the chemical oxidation of **1g** with ferrocenium hexafluorophosphate in THF at low temperature. The resulting EPR spectrum was more detailed and better resolved, but could be simulated with a very similar set of hyperfine coupling constants, thus indicating the formation of the same radical (Fig. 6d). Monitoring of the oxidation at low temperature showed that **3**⁺ is already the only radical in solution below -70 °C and we couldn't observe the intermediary formation of **1g**⁺.

More on the high reactivity of NHC radical cations

A closer look at DFT data suggested a possible alternative fate of non-stabilized radicals **1**⁺, besides direct H-abstraction from solvent molecules to afford **1H**⁺. The optimized geometry of **1**⁺ features two CH₃ groups of the 2,6-di(isopropyl)phenyl (Dipp) *N*-substituents in close vicinity to the carbene radical centre (Fig. 7a). The short H_{CH₃}–C_{carbene} distances (about 230 pm) indicated a possible interaction. This assumption was confirmed by an NBO second-order perturbation energy analysis, which indicated hyper-conjugations of the σ_{C–H}^{*} anti-bonding MO with the singly-occupied carbene “lone pair” (1.7 kcal mol⁻¹), as well as of the σ_{C–H} bonding MO with a vacant C-centred p-orbital (1.9 kcal mol⁻¹). Although most of the spin density is located on the C_{carbene} atom, the two methyl groups bear 3% residual spin density each. Accordingly, **1**⁺ is predicted to evolve straight away to distonic

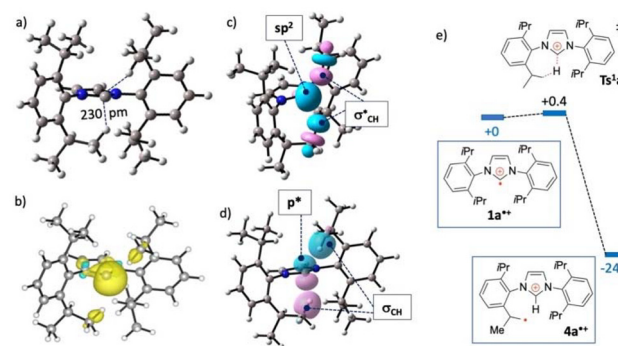


Fig. 7 (a) Optimized geometry of **1**⁺ at the B3LYP-GD3(BJ)/def2svp level of theory. (b) Representation of spin density. (c) Representation of natural molecular orbitals: C-centred sp² SOMO and vacant σ_{CH} (1.7 kcal mol⁻¹ second order interaction), and (d) C-centred vacant p orbital and occupied σ_{CH} (1.9 kcal mol⁻¹). (e) Computed rearrangement of **1**⁺ into **4**⁺ (free enthalpies in kcal mol⁻¹).

alkyl radical **4**⁺, through an almost barrierless H-migration from the methyl to the carbene centre (Fig. 7e).

Although a similar C–H interaction couldn't be found in the optimized structure of NHC radical cations **1b–e**⁺, H-migrations to the carbene radical cation centre from CH₃ and/or CH groups of isopropyl substituents, were found again nearly barrierless ($\Delta G^\ddagger < +5.3$ kcal mol⁻¹) and exergonic (Fig. 8). In all instances, the π-delocalized benzyllic radicals **5**⁺ are the most stable isomer. Importantly, in the case of Dipp *N*-substituents, alkyl radicals **4**⁺ are found to be more stable than NHC radical cation isomers **1**⁺. This is in line with the computed RSE values, which already indicated a lower stability of **1a–e**⁺ compared to the highly reactive methyl radical.

Despite its stabilizing scaffold, the evolution of NHC radical cation **1f**⁺ into isomers **4f**⁺ and **5f**⁺ remain thermodynamically favoured ($\Delta G = -3.6$ and -17.5 kcal mol⁻¹, respectively). The most stabilized oxyallyl-based radical cation

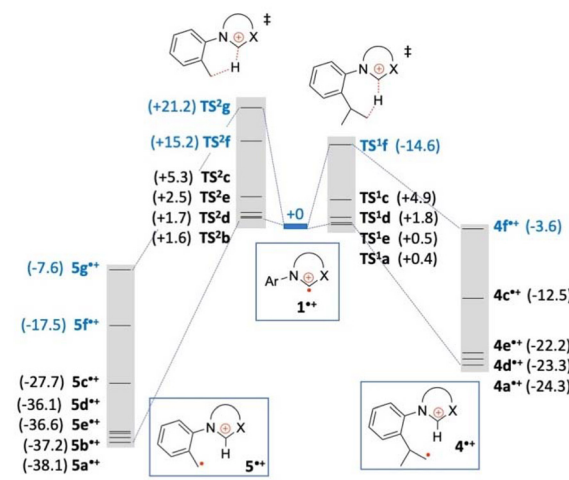


Fig. 8 Computed rearrangement of NHCs **1**⁺ into distonic alkyl radicals **4**⁺ and benzyllic radicals **5**⁺ (free enthalpies in kcal mol⁻¹).



1g⁺ is more reluctant toward H-migration, with a nearly athermic formation of **5g⁺**. This rearrangement is likely the first step to the formation of **3⁺**.

It corresponds to a rather significant computed activation barrier (above 20 kcal mol⁻¹), which suggests that **1g⁺** may perhaps be detectable in cryogenic conditions or in the gas phase.

Dicationic dimers as sources of radicals

Overall, our results showed that NHC radical cations **1⁺** must be extremely short-lived intermediates in solution. They are very unlikely to be involved as radical catalysts, unless they could be generated from resting state species, such as their dimer **2²⁺**. BDE values also indicated that bulkiness does not significantly favour the homolytic dissociation of dicationic dimers **2²⁺**. In addition, we considered that efficient intermolecular trapping had better chances with NHC radical cations **1⁺** with minimal steric hindrance. Thus, we synthesized dicationic dimers **2a²⁺**, **2e²⁺** and **2h²⁺** (based on *N*-methyl substituted imidazolium, *N*-methyl substituted benzimidazolium patterns and a thiazolium respectively), whose bis(hexafluorophosphate) salts are readily accessible by oxidation of the corresponding NHC dimer **2**.^{16c,28}

We found dication **2a²⁺** and **2h²⁺** to be thermally stable. We couldn't evidence any decay after heating an acetonitrile solution under reflux overnight. EPR-monitoring did not indicate the formation of radical traces even when setting the spectrometer temperature up to 70 °C. We also heated acetonitrile solutions in presence of an excess (5 equivalents) of phenyl *N*-*tert*-butylnitrone (PNB, a classical spin trap) at 80 °C. In the case of **2a²⁺**, the crude solution featured a broad EPR spectrum (Fig. 9a). The formation of undetermined radicals may result from decomposition of the radical adducts of PNB. In the case of **2h²⁺**, the EPR spectrum featured a triplet of doublet with hyperfine coupling constants of $a(^{14}\text{N}) = 38.2$ MHz and $a(^1\text{H}) = 5.1$ MHz, that are typical of nitroxide radicals stemming from PNB.²⁹

In marked contrast, the EPR monitoring of a solution **2e²⁺** in acetonitrile indicated the formation of a radical within minutes at 80 °C. The hyperfine structure could be simulated with the same coupling constants as the known^{4b} radical cation **2e⁺** (Fig. 9b). No additional radical could be observed when heating in presence of excess PNB spin-trap. The identity of radical **2e⁺** was further supported by a strong UV-vis absorption at 450 nm and a remarkable air persistency.^{4b}

The formation of **2e⁺** could be due to the generation of **1e⁺** from the homolytic cleavage of **2e²⁺**. Indeed **1e⁺** is prone to fast H⁺ abstraction from the solvent, affording thiazolium **1e⁺H⁺**. This latter could trap another transient radical cation **1e⁺**, affording **2e⁺** after deprotonation (Fig. 10a). Note that the formal addition of H⁺ provides for the reductive event that is required for the formation of **2e⁺** from **2e²⁺** (the carbonic carbon evolves from C^{III} in **1e⁺** to C^{II} in **1e⁺H⁺**). We also considered an alternative: the heterolytic cleavage of **2e²⁺**, which would afford a formal disproportionation of **2e²⁺** (C^{III} carbonic carbon) into the carbene **1e** (C^{II}) and the carbene dication **1e²⁺**.

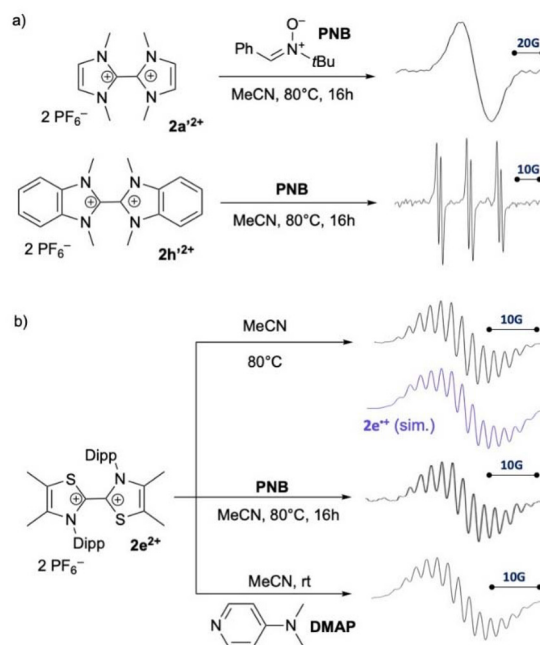


Fig. 9 (a) Generation of radicals from **2a²⁺** and **2h²⁺**; EPR spectra of crude mixture. (b) Generation of **2e⁺**; simulated EPR spectrum with Lorentzian line-broadening parameter $L_w = 0.24$, hyperfine coupling constants $a(^{14}\text{N}) = 11.6$ MHz (2 nuclei) and $a(^1\text{H}) = 6.0$ MHz (6 nuclei).

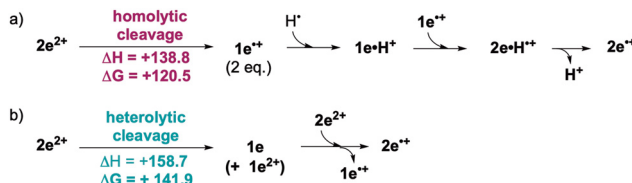


Fig. 10 Possible reductive events for the formation of **2e⁺** from **2e²⁺**: (a) H⁺ abstraction from solvent by **1e⁺** to afford **1e⁺H⁺**, (b) disproportionation of **2e²⁺** into **1e²⁺** and **1e**. Energies are in kcal mol⁻¹ (B3LYP-GD3 (BJ)/def2svp with SMD model for acetonitrile as solvent).

(C^{IV}). NHC **1e** could lead to **2e⁺** by addition to **2e²⁺**, followed by elimination of **1e⁺** (Fig. 10b).

At first, the singularity of **2e²⁺** for the generation of radical seemed inconsistent with the high computed BDE (Fig. 2). When introducing the SMD model for acetonitrile as solvent, the homolytic cleavage was found very endothermic (139 kcal mol⁻¹ Fig. 10a). The heterolytic cleavage was found even less favoured (Fig. 10b). However, the DFT-optimized geometry of **2e²⁺** was unique among dimeric dications **2²⁺**, which usually feature NHC units that are nearly perpendicular, in order to accommodate steric bulk around the central C-C bond. In contrast, in the case of **2e²⁺**, the lack of steric hindrance around the sulphur atom allows both π -systems to be coplanar and conjugated. Importantly, we grew single crystals of a dichloride salt of **2e²⁺** and corroborated the DFT-predicted geometry with an experimental X-ray diffraction study (Fig. 11a). Overall, dication **2e²⁺** features a low-lying LUMO (-9.5 eV) with strong



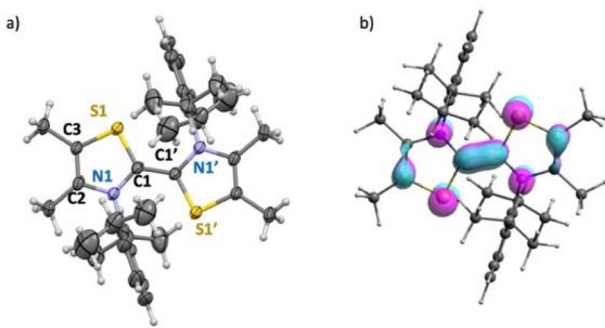


Fig. 11 (a) X-ray crystallographic structure of 2e^{2+} with 40% probability ellipsoids (Cl^- anions are omitted for clarity). (b) Representation of LUMO of 2e^{2+} .

coefficients on the carbon atom of the central C–C bond, which is moderately sterically confined. In line with a superior electrophilicity of 2e^{2+} , the reduction potential of this dication (-0.06 V vs. SCE)^{4b} is significantly higher than that of 2h^{2+} (-0.8 V) and 2a^{2+} (-1.4 V).²⁸

Considering that the resulting peculiar electrophilicity must be linked to its distinctive radical behaviour, we reacted 2e^{2+} with DMAP (a prototypical nucleophilic pyridine) at room temperature. The solution immediately turned red and EPR spectroscopy indicated the formation of 2e^{+} (Fig. 9b). Importantly, no formation of radicals was observed when adding DMAP to an acetonitrile solution of 2a^{2+} or 2h^{2+} , even when heating up to 80 °C. This was in line with the lower electrophilicity of these dication.

Radical generation upon addition of DMAP to 2e^{2+} suggested that Lewis bases could ease the dissociation of the dication, mirroring the acid-catalysed generation of NHCs from their dimers 2 in the Wanzlick equilibrium. Without DMAP, radicals were generated but at a higher temperature. We presumed that the acetonitrile solvent was also able to add to 2e^{2+} and to promote the dissociation of the dication. We probed this hypothesis with DFT calculations with the SMD solvation model. The addition of acetonitrile to 2e^{2+} is endothermic by $\Delta H = 36$ kcal mol⁻¹ and endergonic by $\Delta G = 48$ kcal mol⁻¹ (Fig. 12). The heterolytic cleavage of the acetonitrile adduct is largely favoured over the homolytic cleavage ($\Delta G = 47$ and 20 kcal mol⁻¹ respectively). These values can account for the formation of traces of 2e^{+} at high temperature, via the generation of free NHC **1e**.

In the case of DMAP, addition of the nucleophile and heterocyclic dissociation are significantly less endergonic ($\Delta G = 19$ and 14 kcal mol⁻¹ respectively). These values are consistent with the generation of 2e^{+} at room temperature, which was evidenced experimentally. Once again, the homolytic dissociation of the adduct was found highly endergonic, but less than the dissociation of 2e^{2+} in absence of Lewis base. We failed to optimize with DFT the geometry of a DMAP adduct with 2a^{2+} or 2h^{2+} . All attempts led to the dissociation of the two partners, supporting our assumption that such adducts are less relevant in the case of other dication 2^{2+} .

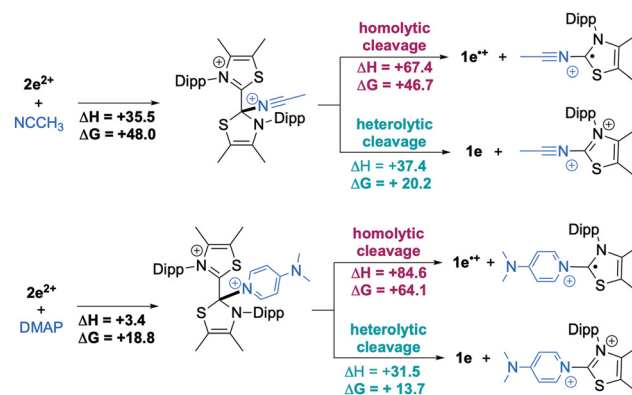


Fig. 12 DFT investigation of the facilitation of the homo- and hetero-dissociations of 2e^{2+} with Lewis bases (B3LYP-GD3(BJ)/def2svp with SMD model for acetonitrile as solvent. Energies are in kcal mol⁻¹.

In conclusion, the formation of 2e^{+} upon heating solution of 2e^{2+} likely involves the heterolytic cleavage of the dication and the formation of free NHC **1e**. This process is promoted by Lewis bases, such as DMAP or the acetonitrile solvent.

Dications 2a^{2+} or 2h^{2+} are far less electrophilic. The generation of radicals from these dications required refluxing for hours. These latter cases may involve the homolytic dissociation of the dication to afford NHC radical cation 1e^{+} . However, EPR is a very sensitive spectroscopy. The fact that harsh conditions are needed for several hours in order to detect radicals through trapping suggests that only insignificant traces are formed.

Dicationic dimers for the initiation of radical chains

NHC radical cations had been postulated as key catalytic intermediates for several parented radical reactions.² The formation of indole 7 through the intramolecular cyclisation of α -bromo amide **6-Br** is a prototypical example (Fig. 13). The reaction can be performed in refluxing 1,4-dioxane in presence of 10% of thiazolium **1e-H⁺** and a base.^{2a} The customary mechanistic proposition involves the formation NHC **1e** and the subsequent reduction of **6-Br** to afford a bromide anion, NHC radical cation 1e^{+} and radical **6**[·]. The latter would undergo an intramolecular cyclisation to afford **7-H[·]** and, then **7^{·-}**, after deprotonation. Finally, the reduction of 1e^{+} by **7^{·-}** would afford the product **7** and regenerate the NHC catalyst **1e** (Fig. 13b). However, in light of our findings, it seemed very unlikely that NHC radical cations could accumulate sufficiently to play the role of an electron shuttle. In addition, we previously reported that 2e^{+} was an efficient promoter of the reaction.^{4b} This was another indication that an alternative radical pathway may be at work.

As a matter of fact, a radical chain could also account for the mechanism.³⁰ Both cyclic voltammograms of **6-Br** and **7** features a reduction wave at around -1.9 V vs. SCE (Fig. 13c). This suggested that **7^{·-}** could enable the propagation of the radical chain by reducing substrate **6-Br** to generate **6**[·] (Fig. 13d).³¹ The fact that this transformation can occur in



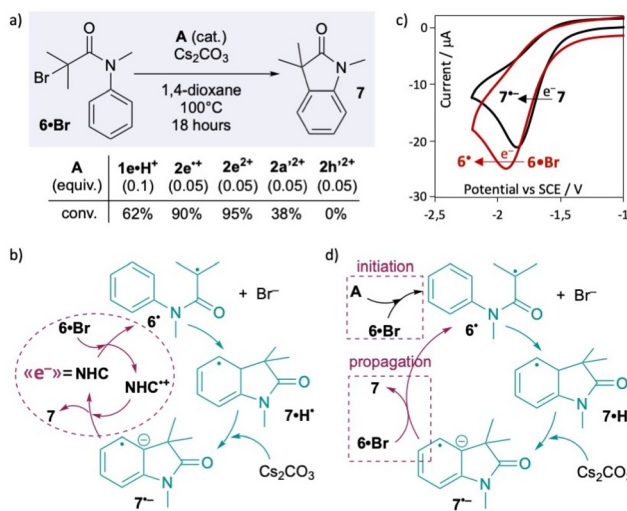


Fig. 13 (a) Radical cyclisation of **6-Br** into oxindole **7**. (b) Customary mechanism involving a NHC catalyst. (c) Cyclic voltammetry of **6-Br** and **7** in acetonitrile + 0.1M $[\text{Bu}_4\text{N}] \text{PF}_6$, scan rate: 100 mV s⁻¹. (d) Proposed radical chain propagation.

presence of radical initiators, such as AIBN and $\text{Bu}_3\text{SnH}^{\bullet}$,³² also supports a radical chain pathway. This alternative mechanistic picture furthermore accounts for the efficiency of poor reducing agents. For instance, although **1e** should undergo oxidative electron transfer above -0.2 V vs. SCE only,^{4b} the subsequent irreversible formation of **1•H⁺** may provide a thermodynamic drive and ultimately allow for the reduction of **6-Br**. Similarly, alternative activation, such as irreversible Br-atom abstraction from **6-Br**, could also benefit from further irreversible exergonic evolution of the initiator.

As dication **2²⁺** could generate radicals in refluxing solutions, we tested **2a²⁺**, **2h²⁺** and **2e²⁺** as radical initiators for the intramolecular cyclisation of **6-Br**. The reaction performed well in presence of 5% of bis(hexafluorophosphate) salt of **2e²⁺** (95% conversion, Fig. 13a). Of course, prior to this study, it would have been tempting to interpret these results as evidence for the transient formation of **1e^{•+}**. However, it is now clear that **2e²⁺** does not undergo homolytic cleavage, but instead generates NHC **1e**, as well as radical **2e^{•+}**, which are both efficient promoters of the reaction.

No conversion was obtained with **2h²⁺** as initiator. Dication **2a²⁺** afforded a modest 38% conversion. In the latter case, it is not possible to totally rule out the homo-dissociation of the dication and the involvement of radical cation **1a^{•+}**.

Conclusions

Our results showcase the high reactivity and elusiveness of radicals **1^{•+}**. Typical NHC radical cations are C_{sp^2} -centered. They are predicted to be extremely short-lived, even in the gas phase, as they can undergo nearly barrierless rearrangements through H atom migration. Spin density delocalization can be achieved with NHC **1f** and **1g**, which feature electron-rich pat-

terns: a bis(dimethylamino)-substituted ethylene and oxyallyl, respectively. However, the radical cations **1f^{•+}** and **1g^{•+}** remain too reactive for direct observation in solution, despite their redox-active ancillary frameworks.

It is clear that the geometric constraints of the N-heterocyclic structure in **1^{•+}** preclude any efficient stabilisation by +M substituents. Future observation or isolation of a radical cation with divalent C^{III} centres will certainly require acyclic structures. Incidentally, Bertrand and co-workers recently reported a stable carbene dication stemming from an acyclic framework.³³ This compound undergoes 2-electron reductions to afford the corresponding neutral form. Although the radical cation may disproportionate in this specific case, one could foresee that a stable version could be designed through structural tuning.

In the course of our study, radicals were observed by EPR on several occasions, when attempting the oxidation of **1g** or the cleavage of dicationic dimers **2²⁺**. Furthermore, **2e²⁺** is an efficient initiator for the radical intramolecular cyclisation of **6-Br**. Each time, it would have been tempting to infer the formation of the desired NHC radical cation **1^{•+}**. However, each time, the formation and/or observation of **1^{•+}** could be dismissed. Indeed, we showed that the oxidation of **1g** afforded oxyallyl radical **3^{•+}**. In addition, bond dissociation energies of dicationic dimers are very high. Although **2a²⁺** or **2h²⁺** may undergo homolytic dissociation in harsh conditions, only the formation of trace amounts of unidentified radicals could be evidenced. Finally, Lewis bases considerably ease the heterolytic dissociation of **2e²⁺**, which leads ultimately to reduced products **1e** and **2e^{•+}** (which promote the formation of **7**), and not to the desired NHC radical cation **1^{•+}**.

In 2023, Song and Lee proposed an alternative mechanism for the reduction of the trityl cation by NHC **1a** and showed that the formal oxidation of the NHC **1** into **1•H⁺** does not necessarily imply the formation of the radical intermediate **1^{•+}**.¹⁰ Our study clearly drives the point home: N-heterocyclic carbene radical cations **1^{•+}** are certainly irrelevant in most radical transformations. Future mechanistic considerations on reductive processes involving free NHCs should systematically look for alternative pathways.

Author contributions

E. T.-M., J. B. and D. M.: conceived the project and acquired funding, provided resources and supervised the project; P. S., L. D., S. B., F. M.: (advanced electrochemical analysis); J. P.: (X-ray diffraction analysis) and D. M.: (DFT calculations) conducted the investigation and formal analysis of the methodology.

All authors contributed to the reviewing and editing of the manuscript.

Conflicts of interest

There are no conflicts to declare.



Data availability

The data supporting this article have been included as part of the supplementary information (SI). Supplementary information is available. See DOI: <https://doi.org/10.1039/d5qo01285f>.

CCDC 2475077 (2e-Cl₂) contains the supplementary crystallographic data for this paper.³⁴

Acknowledgements

This work was funded by the French National Agency for Research (ANR-20-CE07-0010). P. Smits acknowledges Labex Arcane and CBHEUR-GS (ANR-17-EURE-0003) for funding. We thank the CECCIC centre of Grenoble for computer resources and the ICMG analytic platform (FR 2607).

References

- For reviews, thematic issues and books on stable carbenes, see: (a) A. J. Arduengo and G. Bertrand, Carbenes Introduction, *Chem. Rev.*, 2009, **109**, 3209–3210; (b) *N-Heterocyclic Carbene in Transition Metal Catalysis and Organocatalysis*, ed. C. S. J. Cazin, Springer, London, 2011; (c) *N-Heterocyclic Carbenes: From Laboratory Curiosities to Efficient Synthetic Tools*, ed. S. Díez-González, Royal Society of Chemistry Publishing, Cambridge, 2011; (d) T. Rovis and S. P. Nolan, Stable Carbenes: From 'Laboratory Curiosities' to Catalysis Mainstays, *Synlett*, 2013, 1188–1189; (e) *N-Heterocyclic Carbenes—Effective Tools for Organometallic Synthesis*, ed. S. P. Nolan, Wiley-VCH, Weinheim, 2014; (f) M. N. Hopkinson, C. Richter, M. Schedler and F. Glorius, *Nature*, 2014, **510**, 485–496; (g) L. Benhamou, E. Chardon, G. Lavigne, S. Bellemain-Lapoumaz and V. César, Synthetic Routes to N-Heterocyclic Carbene Precursors, *Chem. Rev.*, 2011, **111**, 2705–2733.
- (a) C. Wang and L. Liu, NHC-catalyzed oxindole synthesis via single electron transfer, *Org. Chem. Front.*, 2021, **8**, 1454–1460; (b) L. Su, H. Sun, J. Liu and C. Wang, Construction of Quaternary Carbon Center via NHC Catalysis Initiated by an Intermolecular Heck-Type Alkyl Radical Addition, *Org. Lett.*, 2021, **23**, 4662–4666; (c) L. Liu, C.-Y. Zhou and C. Wang, Construction of highly congested quaternary carbon centers by NHC catalysis through dearomatization, *Green Synth. Catal.*, 2023, **4**, 263–267; (d) Q. Li, C.-Y. Zhou and C. Wang, Divergent Construction of Heterocycles by SOMOphilic Isocyanide Insertion under N-Heterocyclic Carbene Catalysis, *Org. Lett.*, 2022, **41**, 7654–7658; (e) Z. Feng, L. Wu, C.-Y. Zhou and C. Wang, N-Heterocyclic Carbene Catalysis for Polycyclic Benzazepines Assembly: Regioselective Intramolecular Tandem Radical Cyclization, *Org. Lett.*, 2024, **26**(42), 9068–9072; (f) N. Zhou, F. Zhao, L. Wang, X. Gao, X. Zhao and M. Zhang, NHC-Catalyzed Regioselective Intramolecular Radical Cyclization Reaction for the Synthesis of Benzazepine Derivatives, *Org. Lett.*, 2023, **25**, 6072–6076.
- (a) A. Maiti, B. J. Elvers, S. Bera, F. Lindl, I. Krummenacher, P. Ghosh, H. Braunschweig, C. B. Yildiz, C. Schulzke, H.-G. Korth and A. Jana, Comment on "Disclosing CAACs as a One-Electron Reductant: Synthesis of Acyclic(Amino)(Aryl) Carbene-Based Kekulé Diradicaloids", *Chem. – Eur. J.*, 2023, **29**, e202302848; (b) A. Maiti, B. J. Elvers, S. Bera, F. Lindl, I. Krummenacher, P. Ghosh, H. Braunschweig, C. B. Yildiz, C. Schulzke and A. Jana, Disclosing CAACs as a One-Electron Reductant: Synthesis of Acyclic(Amino)(Aryl) Carbene-Based Kekulé Diradicaloids, *Chem. – Eur. J.*, 2022, **28**, e202104567.
- (a) M. Feroci, I. Chiarotto, F. D'Anna, F. Gala, R. Noto, L. Ornano, G. Zollo and A. Inesi, N-Heterocyclic Carbenes and Parent Cations: Acidity, Nucleophilicity, Stability, and Hydrogen Bonding—Electrochemical Study and Ab Initio Calculations, *ChemElectroChem*, 2016, **3**, 1133–1141; (b) L. Delfau, N. Assani, S. Nichilo, C. Philouze, J. Broggi, D. Martin and E. Tomás-Mendivil, On the Redox Properties of the Dimers of Thiazol-2-ylidene That Are Relevant for Radical Catalysis, *ACS Org. Inorg. Au*, 2023, **3**, 136–142.
- (a) T. Ramnial, I. McKenzie, B. Gorodetsky, E. M. W. Tsang and J. A. C. Clyburne, *Chem. Commun.*, 2004, 1054–1055; (b) V. V. Pavlishchuk and A. W. Addison, Conversion constants for redox potentials measured versus different reference electrodes in acetonitrile solutions at 25 °C, *Inorg. Chim. Acta*, 2000, **298**, 97–102.
- Z. Dong, C. Pezzato, A. Sienkiewicz, R. Scopelliti, F. Fadaei-Tirani and K. Severin, SET processes in Lewis acid–base reactions: the tritylation of N-heterocyclic carbenes, *Chem. Sci.*, 2020, **11**, 7615–7618.
- See also: A. C. Shaikh, J. M. Veleta, J. Moutet and T. L. Gianetti, Trioxatriangulenium (TOTA⁺) as a robust carbon-based Lewis acid in frustrated Lewis pair chemistry, *Chem. Sci.*, 2021, **12**, 4841–4849.
- R. Jazza, R. D. Dewhurst, J.-B. Bourg, B. Donnadieu, Y. Canac and G. Bertrand, Intramolecular "Hydroiminiumation" of Alkenes: Application to the Synthesis of Conjugate Acids of Cyclic Alkyl Amino Carbenes (CAACs), *Angew. Chem., Int. Ed.*, 2007, **46**, 2899–2902.
- (a) M. Abdellaoui, K. Oppel, A. Vianna, M. Soleilhavoup, X. Yan, M. Melaimi and G. Bertrand, 1 H-1,2,3-Triazol-5-ylidene as Catalytic Organic Single-Electron Reductants, *J. Am. Chem. Soc.*, 2024, **146**, 2933–2938; (b) J. Bouffard, B. K. Keitz, R. Tonner, G. Guisado-Barrios, G. Frenking, R. H. Grubbs and G. Bertrand, Synthesis of Highly Stable 1,3-Diaryl-1H-1,2,3-triazol-5-ylidene and Their Applications in Ruthenium-Catalyzed Olefin Metathesis, *Organometallics*, 2011, **30**, 2617–2627.
- H. Song and E. Lee, Revisiting the Reaction of IPr with Tritiylium: An Alternative Mechanistic Pathway, *Chem. – Eur. J.*, 2023, **29**, e202203364.
- (a) H.-W. Wanzlick and E. Schikora, Ein nucleophiles Carben, *Chem. Ber.*, 1961, **94**, 2389–2393;



(b) H.-W. Wanzlick, Aspects of Nucleophilic Carbene Chemistry, *Angew. Chem., Int. Ed. Engl.*, 1962, **1**, 75–80; (c) H.-W. Wanzlick, F. Esser and H.-J. Kleiner, Nucleophile Carben-Chemie, III. Neue Verbindungen vom Typ des Bis-[1,3-diphenyl-imidazolidinylidens-(2)], *Chem. Ber.*, 1963, **96**, 1208–1212.

12 For the synthesis of NHC-metal complexes from NHC dimers, see reviews: (a) M. F. Lappert, The coordination chemistry of bivalent group IV donors: Nucleophilic carbene and dialkylstannylene complexes, *J. Organomet. Chem.*, 1975, **100**, 139–159; (b) M. F. Lappert, The coordination chemistry of electron-rich alkenes (enonetetramines), *J. Organomet. Chem.*, 1988, **358**, 185–214; (c) T. Weskamp, V. P. W. Böhm and W. A. Herrmann, N-Heterocyclic carbenes: state of the art in transition-metal-complex synthesis, *J. Organomet. Chem.*, 2000, **600**, 12–22.

13 (a) J. Castells, F. Lopez-Calahorra, F. Geijo, R. Perez-Dolz and M. Bassedas, The benzoin condensation catalysis by bis(azolin-2-ylidene)s and bis(azolidin-2-ylidene)s and its interpretation within the context of nucleophilic carbene chemistry, *J. Heterocycl. Chem.*, 1986, **23**, 715–720; (b) J. Castells, F. Lopez-Calahorra and L. Domingo, Postulation of bis(thiazolin-2-ylidene)s as the catalytic species in the benzoin condensation catalyzed by a thiazolium salt plus base, *J. Org. Chem.*, 1988, **53**, 4433–4436.

14 V. P. W. Böhm and W. A. Herrmann, The “Wanzlick Equilibrium”, *Angew. Chem., Int. Ed.*, 2000, **39**, 4037–4038.

15 (a) F. E. Hahn, L. Wittenbecher, D. Le Van and R. Fröhlich, *Angew. Chem., Int. Ed.*, 2000, **39**, 541–544; (b) J. Messelberger, M. Kumar, S. J. Goodner and D. Munz, *Org. Chem. Front.*, 2021, **8**, 6663–6669.

16 (a) Y. Liu, P. E. Lindner and D. M. Lemal, Thermodynamics of a Diaminocarbene–Tetraaminoethylene Equilibrium, *J. Am. Chem. Soc.*, 1999, **121**, 10626–10627; (b) A. Poater, F. Ragone, S. Giudice, C. Costabile, R. Dorta, S. P. Nolan and L. Cavallo, Thermodynamics of N-Heterocyclic Carbene Dimerization: The Balance of Sterics and Electronics, *Organometallics*, 2008, **27**, 2679–2681; (c) P. I. Jolly, S. Zhou, D. W. Thomson, J. Garnier, J. A. Parkinson, T. Tuttle and J. A. Murphy, Imidazole-derived carbenes and their elusive tetraazafulvalene dimers, *Chem. Sci.*, 2012, **3**, 1675–1679.

17 (a) A. J. Arduengo III, J. R. Goerlich and W. J. Marshall, A Stable Thiazol-2-ylidene and Its Dimer, *Liebigs Ann./Recl.*, 1997, 365–374; (b) R. W. Alder, M. E. Blake, L. Chaker, J. N. Harvey, F. Paolini and J. Schütz, When and How Do Diaminocarbenes Dimerize?, *Angew. Chem., Int. Ed.*, 2004, **43**, 5896–5911; (c) R. W. Alder, L. Chaker and F. P. V. Paolini, Bis(diethylamino)carbene and the mechanism of dimerisation for simple diaminocarbenes, *Chem. Commun.*, 2004, 2172–2173; (d) D. C. Graham, K. J. Cavell and B. F. Yates, Dimerization mechanisms of heterocyclic carbenes, *J. Phys. Org. Chem.*, 2005, **18**, 298–309; (e) D. Martin, N. Lassauque, B. Donnadieu and G. Bertrand, A Cyclic Diaminocarbene with a Pyramidalized Nitrogen Atom: A Stable N-Heterocyclic Carbene with Enhanced Electrophilicity, *Angew. Chem., Int. Ed.*, 2012, **51**, 6172–6175; (f) L. Delfau, J. Pecaut, E. Tomás-Mendivil and D. Martin, Improved Protocols for the Synthesis of Precursors of Thiazol-2-ylidene N-Heterocyclic Carbenes, *Synlett*, 2024, 2097–2100.

18 (a) J. Broggi, T. Terme and P. Vanelle, Organic Electron Donors as Powerful Single-Electron Reducing Agents in Organic Synthesis, *Angew. Chem., Int. Ed.*, 2014, **53**, 384–413; (b) J. A. Murphy, Discovery and Development of Organic Super-Electron-Donors, *J. Org. Chem.*, 2014, **79**, 3731–3746; (c) E. Doni and J. A. Murphy, Evolution of neutral organic super-electron-donors and their applications, *Chem. Commun.*, 2014, **50**, 6073–6087.

19 (a) Z. Shi and R. P. Thummel, Bridged bibenzimidazolium salts and their conversion to ureaphanes, *Tetrahedron Lett.*, 1994, **35**, 33–36; (b) K. Nagata, T. Itoh, M. Okada and A. Ohsawa, The reaction of benzimidazolium derivatives with superoxide, *Tetrahedron*, 1996, **52**, 6569–6580.

20 For examples, see: (a) F. G. Bordwell and T. Y. Lynch, Radical stabilization energies and synergistic (captodative) effects, *J. Am. Chem. Soc.*, 1989, **111**, 7558–7562; (b) J. Hioe and H. Zipse, Radical stability and its role in synthesis and catalysis, *Org. Biomol. Chem.*, 2010, **8**, 3609–3617; (c) A. S. Menon, D. J. Henry, T. Bally and L. Radom, Effect of substituents on the stabilities of multiply-substituted carbon-centered radicals, *Org. Biomol. Chem.*, 2011, **9**, 3636–3657.

21 Calculations were performed with the Gaussian suite of programs: M. J. Frisch, G. W. Trucks, H. B. Schlegel, G. E. Scuseria, M. A. Robb, J. R. Cheeseman, G. Scalmani, V. Barone, G. A. Petersson, H. Nakatsuji, X. Li, M. Caricato, A. V. Marenich, J. Bloino, B. G. Janesko, R. Gomperts, B. Mennucci, H. P. Hratchian, J. V. Ortiz, A. F. Izmaylov, J. L. Sonnenberg, D. Williams-Young, F. Ding, F. Lipparini, F. Egidi, J. Goings, B. Peng, A. Petrone, T. Henderson, D. Ranasinghe, V. G. Zakrzewski, J. Gao, N. Rega, G. Zheng, W. Liang, M. Hada, M. Ehara, K. Toyota, R. Fukuda, J. Hasegawa, M. Ishida, T. Nakajima, Y. Honda, O. Kitao, H. Nakai, T. Vreven, K. Throssell, J. A. Montgomery Jr, J. E. Peralta, F. Ogliaro, M. J. Bearpark, J. J. Heyd, E. N. Brothers, K. N. Kudin, V. N. Staroverov, T. A. Keith, R. Kobayashi, J. Normand, K. Raghavachari, A. P. Rendell, J. C. Burant, S. S. Iyengar, J. Tomasi, M. Cossi, J. M. Millam, M. Klene, C. Adamo, R. Cammi, J. W. Ochterski, R. L. Martin, K. Morokuma, O. Farkas, J. B. Foresman and D. J. Fox, *Gaussian 16, Revision B.01*, Gaussian, Inc., Wallingford CT, 2016.

22 (a) S. M. Huber, F. W. Heinemann, P. Audebert and R. Weiss, 4,5-Bis(dialkylamino)-Substituted Imidazolium Systems: Facile Access to N-Heterocyclic Carbenes with Self-Umpolung Option, *Chem. – Eur. J.*, 2011, **17**, 13078–13086; (b) Y. Zhang, V. César, G. Storch, N. Lugan and G. Lavigne, Skeleton Decoration of NHCs by Amino Groups and its Sequential Booster Effect on the Palladium-Catalyzed Buchwald–Hartwig Amination, *Angew. Chem., Int. Ed.*, 2014, **53**, 6482–6486; (c) M. Ruamps, S. Bastin,



L. Rechignat, A. Sournia-Saquet, D. A. Valyaev, J.-M. Mouesca, N. Lughan, V. Maurel and V. César, Unveiling the redox-active character of imidazolin-2-thiones derived from amino-substituted N-heterocyclic carbenes, *Chem. Commun.*, 2018, **54**, 7653–7656; (d) M. Ruamps, S. Bastin, L. Rechignat, A. Sournia-Saquet, L. Vendier, N. Lughan, J.-M. Mouesca, D. A. Valyaev, V. Maurel and V. César, Redox-Switchable Behavior of Transition-Metal Complexes Supported by Amino-Decorated NHCs, *Molecules*, 2022, **27**, 3776.

23 E. Tomás-Mendivil, M. Devillard, V. Regnier, J. Pecaut and D. Martin, Air-Stable Oxyallyl Patterns and a Switchable NHC, *Angew. Chem., Int. Ed.*, 2020, **59**, 11516–11520.

24 (a) V. Regnier and D. Martin, The quest for observation and isolation of oxyallyl derivatives, *Org. Chem. Front.*, 2015, **2**, 1536–1545; (b) J. K. Mahoney, D. Martin, F. Thomas, C. Moore, A. L. Rheingold and G. Bertrand, Air-Persistent Monomeric (Amino)(carboxy) Radicals Derived from Cyclic (Alkyl)(Amino) Carbenes, *J. Am. Chem. Soc.*, 2015, **137**, 7519–7525; (c) V. Regnier, F. Molton, C. Philouze and D. Martin, A persistent oxyallyl radical cation with simple di(methyl)amino substituents, *Chem. Commun.*, 2016, **52**, 11422–11425; (d) J. L. Peltier, M. R. Serrato, V. Thery, J. Pecaut, E. Tomás-Mendivil, G. Bertrand, R. Jazzar and D. Martin, An air-stable radical with a redox-chameleonic amide, *Chem. Commun.*, 2023, **59**, 595–598.

25 J. Messelberger, A. Grunwald, S. J. Goodner, F. Zeilinger, P. Pinter, M. E. Michlich, F. W. Heinemann, M. M. Hansmann and D. Munz, Aromaticity and sterics control whether a cationic olefin radical is resistant to disproportionation, *Chem. Sci.*, 2020, **11**, 4138–4149.

26 Experimental EPR spectra were fitted with the EasySpin simulation package: S. Stoll and A. Schweiger, EasySpin, a comprehensive software package for spectral simulation and analysis in EPR, *J. Magn. Reson.*, 2006, **178**, 42.

27 (a) T. W. Hudnall and C. W. Bielawski, An N,N'-Diamidocarbene: Studies in C–H Insertion, Reversible Carbonylation, and Transition-Metal Coordination Chemistry, *J. Am. Chem. Soc.*, 2009, **131**, 16039–16041; (b) J. P. Moerdijk, D. Schilter and C. W. Bielawski, Diamidocarbenes: Isolable Divalent Carbons with Bona Fide Carbene Reactivity, *Acc. Chem. Res.*, 2016, **49**, 1458–1468; (c) P. R. Sultane, G. Ahumada, D. Janssen-Mgller and C. W. Bielawski, Cyclic (Aryl)(Amido)Carbenes: NHCs with Triplet-like Reactivity, *Angew. Chem., Int. Ed.*, 2019, **58**, 16320–16325; (d) Z. R. McCarty, D. N. Lastovickova and C. W. Bielawski, A cyclic (alkyl)(amido)carbene: synthesis, study and utility as a desulfurization reagent, *Chem. Commun.*, 2016, **52**, 5447–5450.

28 (a) G. Tintori, A. Fall, N. Assani, Y. Zhao, D. Bergé-Lefranc, S. Redon, P. Vanelle and J. Broggi, Generation of powerful organic electron donors by water-assisted decarboxylation of benzimidazolium carboxylates, *Org. Chem. Front.*, 2021, **8**, 1197–1205; (b) Y. Zhao, M. Rollet, L. Charles, G. Canard, D. Gigmes, P. Vanelle and J. Broggi, Switching from Single to Simultaneous Free-Radical and Anionic Polymerization with Enamine-Based Organic Electron Donors, *Angew. Chem., Int. Ed.*, 2021, **60**, 19389–19396; (c) M. Horner, S. Hünig and H. Pütter, An empirical rule for the estimation of potentials of multistep redox systems, *Electrochim. Acta*, 1982, **27**, 205–214.

29 The NIH Spin Trap Database is available online free of charge: <https://tools.niehs.nih.gov/stdb/index.cfm/spintrap/>.

30 For conceptual equivalences and differences between radical chain reactions and “electron catalysed” reactions, see: (a) A. Studer and D. P. Curran, The electron is a catalyst, *Nat. Chem.*, 2014, **6**, 765–773; (b) O. R. Luca, J. L. Gustafson, S. M. Maddox, A. Q. Fenwick and D. C. Smith, Catalysis by electrons and holes: formal potential scales and preparative organic electrochemistry, *Org. Chem. Front.*, 2015, **2**, 823–848; (c) A. Studer and D. P. Curran, Catalysis of Radical Reactions: A Radical Chemistry Perspective, *Angew. Chem., Int. Ed.*, 2016, **55**, 58–102.

31 M. A. Syroeshkin, F. Kuriakose, E. A. Saverina, V. A. Timofeeva, M. P. Egorov and I. V. Alabugin, Upconversion of reductants, *Angew. Chem., Int. Ed.*, 2019, **58**, 5532–5550.

32 T. Nishio, K. Iseki, N. Araki and T. Miyazaki, Synthesis of Indolones via Radical Cyclization of N-(2-Halogenoalkanoyl)-Substituted Anilines, *Helv. Chim. Acta*, 2005, **88**, 35–41.

33 Y. K. Loh, M. Melaimi, M. Gembicky, D. Munz and G. Bertrand, A crystalline doubly oxidized carbene, *Nature*, 2023, **623**, 66–70.

34 CCDC 2475077: Experimental Crystal Structure Determination, 2025, DOI: [10.5517/ccdc.csd.cc2p2j6j](https://doi.org/10.5517/ccdc.csd.cc2p2j6j).

